

11674-2002

DL/SCI/P 170 A

preprint

Daresbury Laboratory

DL/SCI/P 170 A

THE 5 TESLA SUPERCONDUCTING WIGGLER MAGNET FOR THE SRS

by

D.E. BAYNHAM and P.T.M. CLEE, Rutherford Laboratory;

and

N. MARKS, Daresbury Laboratory.

Presented at the Wiggler Meeting, Frascati, 29-30 June, 1978

FEBRUARY 1979

Science Research Council

Daresbury Laboratory

Daresbury, Warrington WA4 4AD

Lending Copy

Dezernat Washington WVA 410

Dezernat Gerontologiya

Science Research Center

БЕЗУПЛАТНО

Безопасность при проведении работ. Выходит 28-30 июня 1948

И. МУЖИХА, Деzернат Геронтологiya

при

Д.С. ВУДИНГ и др. Д.С. СТЕВ. Эффективность Геронтологiya

ру

При 2 лету содействовались различные материалы по делу

ОГЛАВЛЕНИЕ

Инструкция

Dezernat Gerontologiya

Пеннингтон

ОГЛАВЛЕНИЕ

# THE 5 TESLA SUPERCONDUCTING WIGGLER MAGNET FOR THE SRS

by D.E. BAYNHAM and F.T.M. CLEE  
Science Research Council, Rutherford Laboratory, Chilton,  
Didcot, Oxon OX11 0QX, U.K.

and

N. MARKS  
Science Research Council, Daresbury Laboratory, Daresbury,  
Warrington WA4 4AD, U.K.

## 1. Introduction

The SRS is a 2 GeV electron storage ring now being built at Daresbury as a dedicated source of synchrotron radiation<sup>1,2</sup>. The radiation from the 1.2 T bending magnets has a characteristic wavelength of 3.9 Å. The Science Research Council has approved the construction of a 3-pole transverse superconducting wiggler magnet to enhance the performance of the machine for short wavelength users. Previous work on magnet design has been reported elsewhere<sup>3,4</sup> this paper outlines the present status. The design field at the orbit is 5 T.

The radiation spectrum from the wiggler is shown in fig.1. The flux exceeds that from the normal magnet below 2 Å wavelength, it is an order of magnitude greater below 1 Å, and the effective cut-off is extended to 0.1 Å. Particular fields of research which will benefit from the wiggler includes small angle scattering, x-ray topography, absorption microscopy and EXAFS. Inelastic scattering and non-linear optics are examples of topics which will hardly be possible without the wiggler.

The wiggler will be inserted in a straight section and its effects on the beam dynamics of the storage ring have been calculated and are acceptably small. The beam line planned for the wiggler has a horizontal aperture of 40 mrad and can be up to 43 m long from the tangent point.

## 2. Magnet System

### 2.1 General

The design is based on 3 parallel dipoles, each being an assembly of 'racetrack' type conductor elements. The proposed magnet-cryostat assembly is shown in fig.2. The racetrack coils are arranged with straight sections transverse to the beam direction in order to achieve the short field periodicity; a beam pipe subtending an angle of 40 mrad is consistent with

a field of 5 T over some 60 mm of axial length. The outer 'racetrack' poles have the same physical length as the centre assembly but operate at half magnetic field. The iron yoke contributes approximately 0.5 T of bending field but more importantly truncates the axial field and provides necessary lateral screening. Particular attention has been paid to two machine constraints which dominate the design: the vertical aperture of the magnet and field integral requirements imposed by the SRS.

## 2.2 Vertical Aperture

The performance of the magnet is determined by the peak magnetic field at the superconductor, whilst the field at the beam, which is less, is the significant synchrotron radiation parameter. The vertical magnet aperture largely determines the peak field to bending field ratio ( $B_p/B_0$ ), and therefore it is important to locate the energising coils as close as possible to the beam. In an early design, the magnet cryostat had a warm-bore, and the beam vacuum chamber, with its *in situ* bakeout facilities, was located in this tube. This large aperture limited the magnet to a maximum field, at the beam, of about 4.2 T.

A design that integrates the beam pipe and the magnet cryostat has now been produced. The bore can be heated to 150°C, for vacuum bakeout, whilst the magnet is at, or near, its operating temperature of 4.3°K, and can withstand the differential pressure of one atmosphere at this temperature. This has resulted in a 30% decrease of magnet aperture, and gives a ratio  $B_p/B_0$  of about 1.35. Figure 3 shows the guaranteed performance of the niobium-titanium superconductor at a temperature of 4.35°K, which is achievable with commercially available refrigerators. The magnet peak field and central field load lines are included, showing that with the coil operating at 82% of short sample performance a central field of 5 T

will be realised. It is therefore believed that with the reduced aperture, it is no longer necessary to reduce the temperature of the superconductor below 4.35°K to achieve the design field. Furthermore, from considerations of enthalpy, it appears that if the coils fail to achieve 82% of short sample performance, only very marginal improvements can be made by lowering the temperature. Hence it is not intended to operate the cryostat below atmospheric pressure in order to obtain a reduced temperature.

## 2.3 Field Integral

The computer code GRUN3P<sup>5</sup> has been used to compute the magnetic fields and field integrals in an extensive study of coil-iron geometries and iron saturation effects. Ideally the field integral through the wiggler system should be zero for dipole and harmonic terms. In practice the tolerance on wiggler integral field errors is determined by the correcting power of the adjacent SRS multipole<sup>6,7</sup>.

Initial studies were based on a system of racetrack coils with identical geometry but with the outer low field coils operating at half current density. Without iron this type of coil arrangement satisfied the requirement  $\int B dx = 0$  for both dipole and harmonic terms. Further, if linear iron was included in the form of a sufficiently long yoke the field integral requirement is still satisfied. This type of model has been used to establish the order of computational accuracy and the degree of discreteness required for the iron. In the case of non-linear iron, saturation in the central high field region gives rise to dipole and harmonic integral errors. Racetrack coils with identical current density are more compatible with available construction techniques and offer greater flexibility in performance. The magnet design is therefore centred on full current density coils, see fig. 4A and B. In this type of system field integral errors arise from

both geometrical and iron saturation effects. The calculated variation of field integral with horizontal position (x) has been fitted to the function

$$\int Bdl = \sum_{n=0}^4 a_{2n} x^{2n}$$

and the coefficients ( $a_{2n}$ ) calculated using a standard routine. It was found that the fourteen and eighteen pole terms ( $a_6$  and  $a_8$ ) produced no significant contribution to the wiggler field over its usable horizontal aperture, and the behaviour of the magnet could be described by the dipole, sextupole and decapole coefficients ( $a_0$ ,  $a_2$  and  $a_4$ ) alone. These are shown in fig.5 as a function of central field. The geometrical and iron saturation effects are clearly distinguished. The dipole contribution can be trimmed to zero by adjustment of the outer coil currents which will give rise to small changes in the harmonic amplitudes. An indication is given of the SRS multipole capacity.

Computer calculations have shown that the quadrupole and octupole errors arising from manufacture and assembly should be easily corrected by the multipole.

#### 2.4 Coil Design

The coil design is based on two standard racetrack coil units, which are used to build up the centre and outer coil assemblies. The  $2.2 \times 1.1 \text{ mm}^2$  conductor will be insulated with kapton and the completed coils impregnated with epoxy resin.

The use of standard units to build up the central and outer poles allows flexibility in the choice of the location of each manufactured coil. Of the eight units required to assemble the central pole, only the inner pairs experience the peak field of 6.7 T when the magnet is producing

5.0 T at the beam. Under such conditions, the field at the inner coils in the two outer poles does not exceed 3.4 T. Hence, of the eight inner coils in the magnet, only four are required to operate at 82% of short sample performance, and the standardisation of design will allow the selection of the coils that give the best results on test. Furthermore, if, after having manufactured and tested a number of coils, it appears that none are achieving the required short sample performance, design modifications can be made to the later windings. In particular, small quantities of niobium-tin superconductor can be placed at critical positions in the coil, at little extra cost, and this will lead to a significant reduction in the operating level that is necessary to achieve a 5 T field.

The major mechanical problems in the magnet construction are associated with the restraint of the magnetic forces. The central reactrack coils experience an attractive force of 1 MN/m length of coil. Since the vertical aperture is such an important design constraint it is desirable to reduce the support structure to a minimum. The proposed structure is indicated in fig.4A and B and consists of an aluminium alloy bridge. Calculations have shown that to operate at an acceptable stress level for the material ( $170 \text{ MN/m}^2$ ) it is necessary to reduce the width of the coil section. This is done by splitting the coil section which enables a 10 mm wide supporting rib to be inserted, see fig.4A. The bridge thickness at the coil section is 5 mm, with 6 mm radii at the corners to reduce the stress concentration.

Full lateral support is provided in the straight sections of the coils, for in this direction the thermal contraction of the support material matches that of the coil section. Along the conductor the thermal contraction is less than in the aluminium alloy support due to the niobium-titanium fila-

ments in the superconductor. Therefore, longitudinally there will be no restraints and the end turns will be self-supporting to the radial forces.

### 3. Refrigeration

The magnet will be connected on closed cycle to a refrigerator, which will be used to cool the magnet from 300°K to 4.35°K, taking less than 24 hours. Under running conditions the system will have a cryogenic power loss of 30 W at 4.35°K. The cryostat will have a liquid nitrogen radiation shield to minimize the heat inleak.

### 4. Power Supply

The magnet power supply and protection network is shown in Fig.6. The supply must maintain a programmed balance between the inner and outer coil sections in order to achieve a nominally zero field integral. The main drive current is from PS.1 and trimming of the sections is by PS.2 and PS.3. The voltage limiting elements DR1-DR6 are to protect the magnet and power supplies during quench. This protection requires a system of seven current leads into the cryostat each rated at full current for quench conditions. The current leads contribute ~ 30% to the refrigerator loading.

### 5. Interaction with Beam Dynamics

It is fundamental to the performance of the wiggler that the radiation loss of the storage ring will be increased, and it will therefore be necessary to increase the r.f. over-voltage to preserve the beam lifetime. It also follows that the radiation damping of the beam oscillations in all three dimensions will be increased, leading to marginal decreases in the damping time constants. However, other potentially damaging interactions depend on the detailed magnetic characteristics of the

wiggler and these have been studied.

The magnet has been designed with parallel pole edges and this has the advantage of being non-dispersive and therefore not modifying the off-momentum electron orbits. This also results in the vertical dipole field not interacting with the focusing in the horizontal plane. However, there will be an edge focusing effect in the vertical plane, and this has been analysed using a hard edge model<sup>8</sup>. With the wiggler operating at 5.0 T, an increase in the storage ring's vertical Q value of 0.07 is expected. Furthermore, the presence of such a focusing element at one point only in the machine lattice will lead to increases in the half widths of the nearest integral and half integral vertical resonances (3 and 3.5) by the same amount. It is planned to overcome the increase in focusing by making small changes to the excitation of the lattice quadrupoles to return the beam to the required working point. This, however, will not reduce the stop-band widths.

The design value for the vertical Q value is sufficiently far from the resonances for the enhanced widths not to disturb the beam. If, however, under operating conditions, it is found highly desirable, for other reasons, to choose a working point that is within 0.07 of the integral of half-integral resonance, the immediately adjacent multipole magnet<sup>6,7</sup> will be used to generate a quadrupole field to reduce the resonance width. This will transfer the problem to the horizontal plane, and it is expected that the solution to such difficulties will entail a compromise between the two planes.

It has been shown in Fig.5 that the integrated sextupole and decapole field errors expected from the wiggler are well within the maximum specification of the multipole magnet. In the case of these perturbations, the

harmonic field generated by the local multipole magnet can be used for exact cancellation and hence, interactions with the beam are not expected.

#### 6. Conclusions

Detailed design of the wiggler magnet is nearing completion and present emphasis is centred on the construction programme. The central field of 5 T requires magnet operation of 80-85% of the superconductor rating. In the light of world-wide experience with superconducting magnet systems this level of performance may prove difficult to achieve due to the phenomenon of "training". The magnet construction programme is therefore geared to provide an early performance assessment of the central high field coil assembly. Preliminary calculations have shown that operating levels could be reduced significantly (to 70%) by the inclusion of a small amount of niobium-tin superconductor in the high field region. Magnet completion is scheduled for early 1980.

#### References

1. V.P. Suller and D.J. Thompson, "Progress Report on the 2 GeV Synchrotron Radiation Source (SRS) at Daresbury", Nucl. Instrum. Meths. 152, (1978) 1.
2. SRS Design Group, Daresbury Laboratory Report DL/SRF/R 2 (1975).
3. P.T.M. Clee et al, Rutherford Laboratory Report RL/75/065 (1975).
4. D.E. Baynham, P.T.M. Clee and D.J. Thompson, "A 5 Tesla Wiggler Magnet for the SRS", Nucl. Instrum. Meths. 152, (1978) 31.
5. A.G.A.M. Armstrong et al, "GFUN3D Users Guide", Rutherford Laboratory Report RL/76/029/A (1976).
6. N. Marks, "Multipole Magnets for the Daresbury Synchrotron Radiation Source", Proc. 5th Int. Conf. on Magnet Technology, Frascati, 1975. (Frascati: CNEN, 1975) p.22.
7. N. Marks, "The SRS Prototype Multipole Magnet", Presented at the 6th Int. Conf. on Magnet Technology, Bratislava, 1977.
8. V.P. Suller, "The Wiggler - Its Effect on Beam Dynamics", SRS Group Internal Note, SRS/NS/75/67.

Figure Captions

Figure 1 Synchrotron radiation spectrum from a 1.2 T bending magnet and from the 5.0 T superconducting wiggler magnet.

Figure 2 Cut-away view of the 5.0 T superconducting wiggler magnet.

Figure 3 Superconductor characteristics and central coil load lines.

Figure 4 Geometry of the superconducting wiggler magnet coils and support (A), viewed normally to the direction of the beam; and (B), viewed in the direction of the beam.

Figure 5 Integral field coefficients in the superconducting wiggler magnet as a function of the central field.

Figure 6 Schematic diagram for the power supply and protection network for the superconducting wiggler magnet.

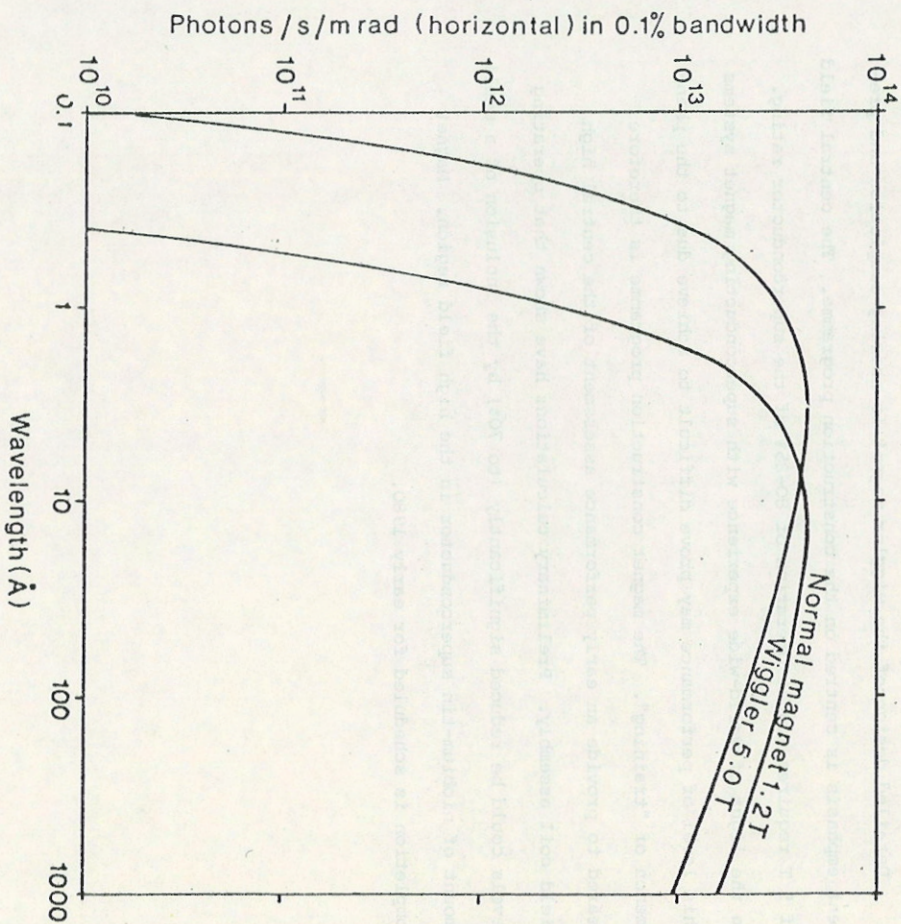


Fig. 1



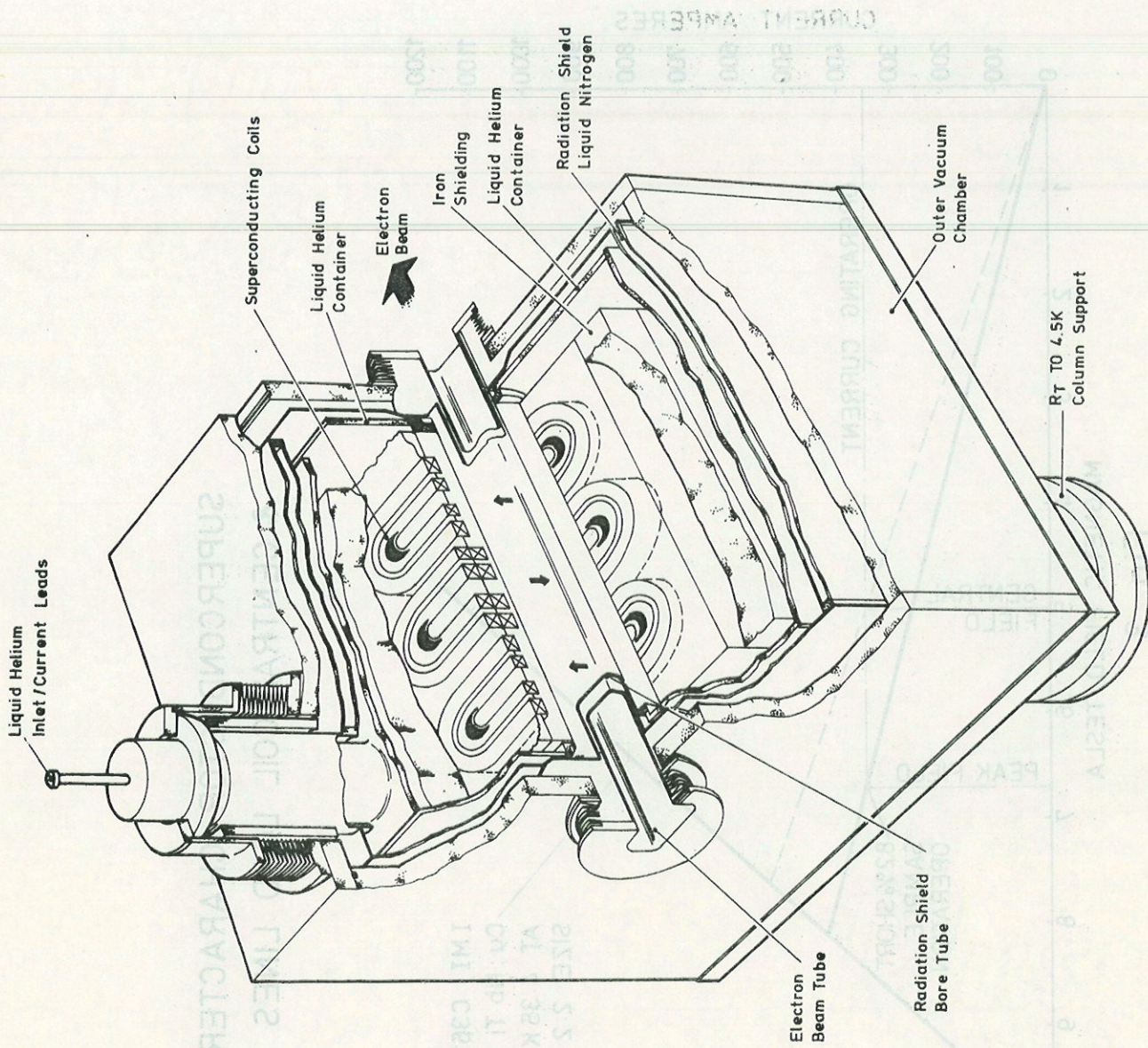


FIG. 2

## SUPERCONDUCTOR CHARACTERISTICS & CENTRAL COIL LOAD LINES

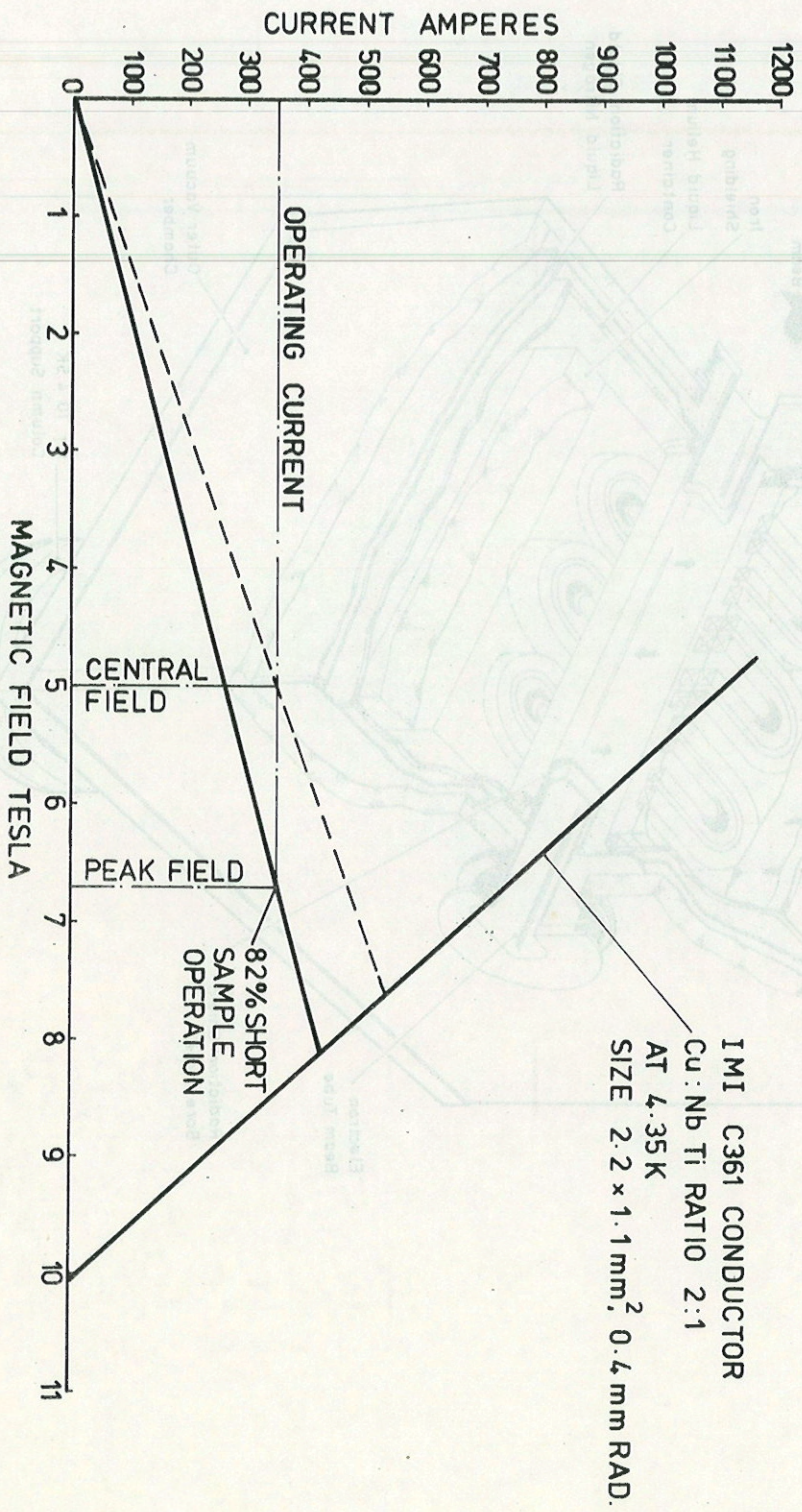
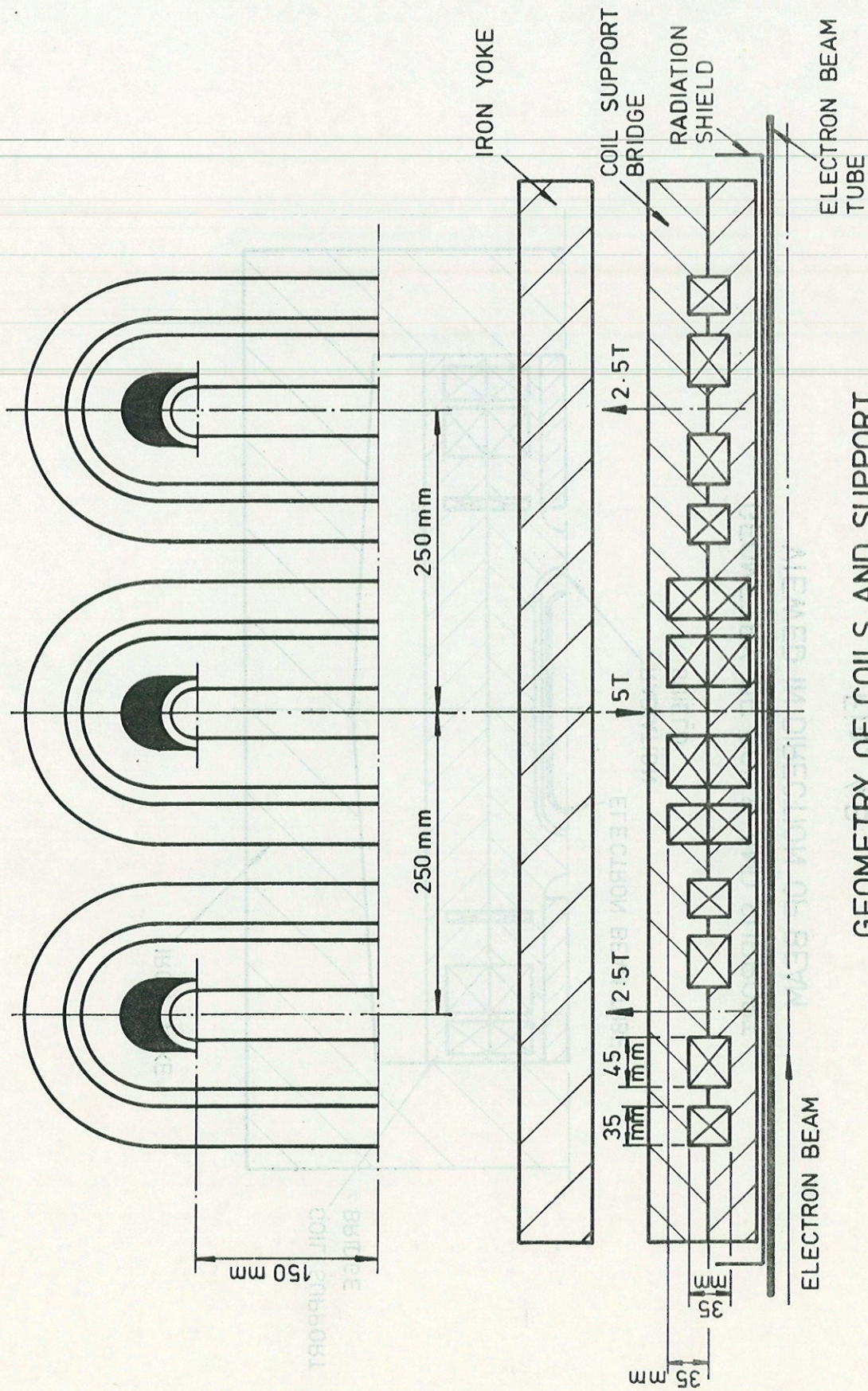


Fig. 3



GEOMETRY OF COILS AND SUPPORT  
 VIEWED NORMAL TO DIRECTION OF BEAM

Fig. 4A

GEOMETRY OF COILS AND SUPPORT  
VIEWED IN DIRECTION OF BEAM

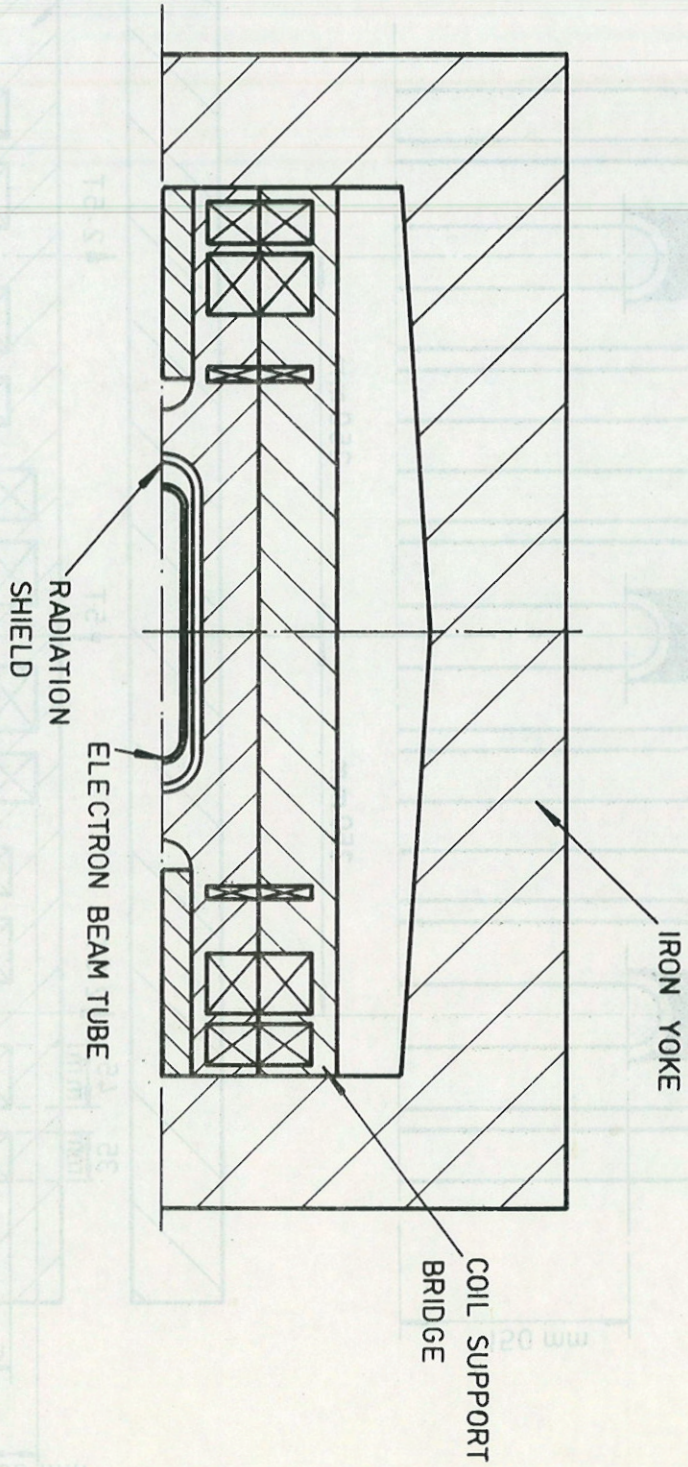


Fig. 4B

# INTEGRAL FIELD COEFFICIENTS VS CENTRAL FIELD

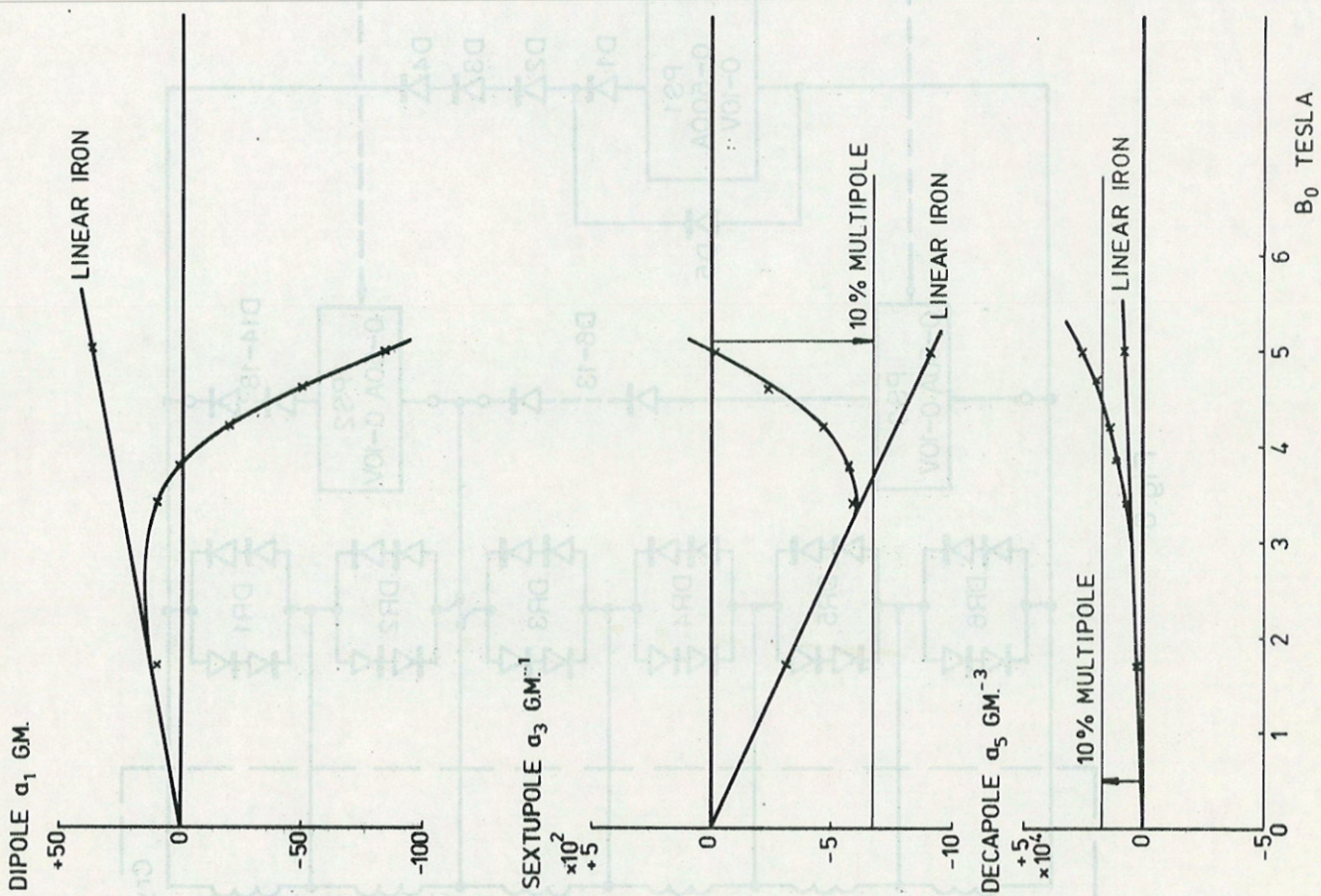


Fig. 5

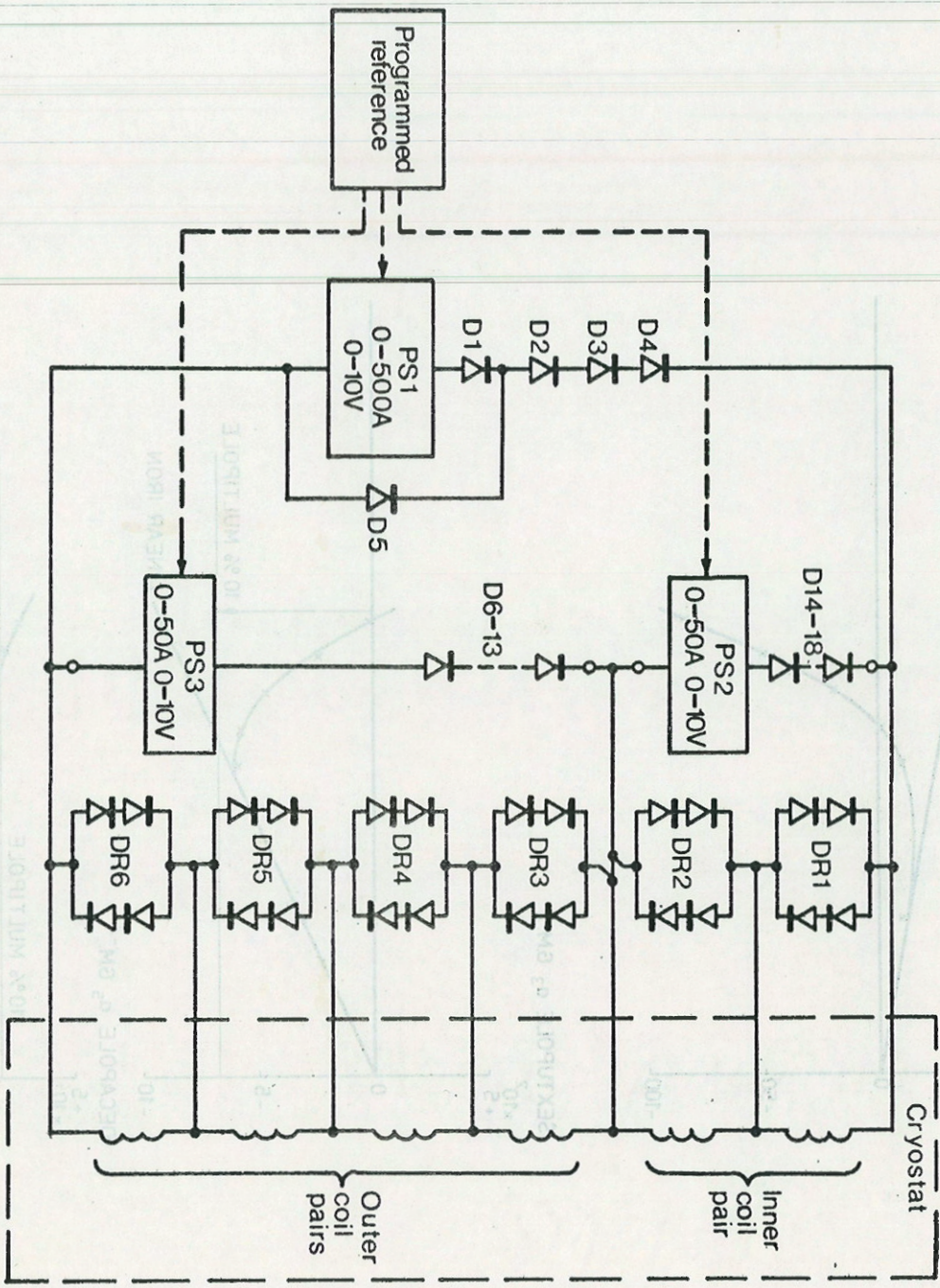


Fig. 6

ИНТЕГРАЛЬНЫЙ КОЭФФИЦИЕНТ ЭФФЕКТИВНОСТИ РАДИОТЕХНИЧЕСКОГО УСТРОЙСТВА